

Ground Deformations in the Very Near Fault Region during the M6.0 South Napa Earthquake

N. Wagner¹, J.D. Bray² and N. Sitar³

ABSTRACT

The M6.0 South Napa earthquake on August 24, 2014 provided a unique opportunity to study very near fault deformations. Initial reconnaissance of the residential neighborhoods in West Napa following the earthquake noted extensive zones of surface deformation, consisting of compression features, including buckled sidewalks, curbs, and pavement. Whereas some deformations were directly associated with surface faulting, much of the observed deformation consisted of compressional features, which occurred away from surface faulting, and could not be attributed to any particular faulting mechanism. One neighborhood with significant effects of surface faulting and well expressed compressive features was chosen for detailed mapping over a three day period, August 26 to 28, 2014. Specifically, compression and extension features along streets and sidewalks parallel to the fault trace and along cross streets roughly orthogonal to the fault trace were measured in detail. A summary of the observations and recordings are discussed in this article.

Introduction

Initial reconnaissance of the residential neighborhoods in West Napa, CA immediately following the earthquake on August 24 and August 25, 2014 noted extensive zones of surface deformations consisting of buckled sidewalks, curbs, and pavement. While some of this deformation was clearly associated with surface faulting, much of the observed deformation consisted of compressional features which could not be directly attributed to any particular faulting mechanism. These features were particularly well expressed in the neighborhood of West Napa bounded by Partrick Road and Browns Valley Road to the north and Buhman Avenue to the east (Figure 1). This area was mapped in detail over a period of three days, August 26 to August 28, 2014. Specifically, measurements were made of compression and extension along streets and sidewalk parallel to the fault trace and along the cross streets, roughly orthogonal to the fault trace (Bray et al. 2015). A summary of these observations and recordings is presented here.

Overview of Ground Strain Observations

A typical buckled compression zone and extension crack is shown in Figure 2. These types of compression features were predominantly concentrated in concrete sidewalks and were quite

¹PhD Candidate, Civil & Environmental Engineering, UC Berkeley, Berkeley, CA, USA, nbwagner@berkeley.edu

²Faculty Chair in Earthquake Engineering Excellence, Civil & Environmental Engineering, UC Berkeley, Berkeley, CA, USA, jonbray@berkeley.edu

³Edward G. Cahill and John R. Cahill Professor, Civil & Environmental Engineering, UC Berkeley, Berkeley, CA, USA, sitar@berkeley.edu

readily apparent while extension cracks were typically quite innocuous and required a careful inspection. It should be noted that frequently there was no evidence of similar deformation in the adjacent bituminous pavement in the street.

Measurement methodology

A consistent measurement procedure was used in the field to standardize the observations of compression zones and extension cracks. First, a 100 meter tape measure with 1 millimeter increments was stretched in the road parallel to the sidewalk approximately 2 meters from the edge of the curb and divided into 25 meter segments. This configuration was chosen because the roads were well paved and essentially free of distortion (primarily tree root uplift and buckled sidewalk pavement, etc.) that would cause the 25 meter segment to be shorter than it should actually have been. The ends of the 25 meter segment were marked with spray paint and numbered, and then the bearing along the segment was estimated with a compass. At intersections, the segment measurement was continued until the concrete curb contacted the asphalt and the reduced (or augmented) segment length was recorded.

Next, the sidewalk in the segment was carefully inspected and the compression zones and extension cracks were measured relative to the start of the segment. Extension cracks were measured to the nearest 1 mm with a ruler or tape measure perpendicular to the crack at various locations, and then a representative value was reported. When possible, area residents were consulted as to which cracks existed prior to the earthquake. Small cracks filled with debris (<1 mm) were not considered since debris-filled cracks were observed with a modest (up to 3 mm) gap on at least one side. This indicated that the debris-filled cracks with no gaps were not due to the earthquake. Additionally, cracks in sidewalk pavement that had been previously ground down were not considered. These cracks were often in expansion joints and had been shaved to offer a smoother transition between uplifted sections of pavement.

Deformation in the buckled compression zones was assessed by first measuring the lengths of the uplifted sidewalk section along the top surface on the same edge to obtain the original length of the section. Then, the distance between the new outer edges of the sidewalk was measured to obtain the new length of the section. The difference between the measurements was recorded as the compression in the zone. Measurements for a typical buckled section are shown in Figure 3.

In some locations, compression in the sidewalk pavement manifested as an overlap instead of a buckled section. In such cases the overlap was measured and recorded as the compression in the zone. The measurement for an overlapping compression zone is shown in Figure 4. In cases where both gaps and overlaps were observed, the gaps were subtracted from the overlap measurement and this value was recorded as the compression in the zone. The measurement for an overlapping compression zone with a gap is shown in Figure 5.



Figure 1: Observation and measurement sections of ground strain (red lines) and approximate observed fault trace (yellow line); produced in Google Earth; [Napa, CA; N 38.3040 W 122.3443; 8/26/14 - 8/28/14]; Bray et al. (2015).



Figure 2: Typical buckled compression zone (left) and extension crack (right) [N 38.3037 W 122.3433; 8/26/2014 15:41 (left); N 38.3055 W 122.3455; 8/26/2014 18:34 (right)]; Bray et al. (2015).



Figure 3: Measuring a typical buckled compression zone in sidewalk pavement [N 38.3039 W 122.3430; 8/26/2014 15:24]; Bray et al. (2015).



Figure 4: Measuring an overlapped compression zone in sidewalk pavement [N 38.3065 W 122.3454; 8/28/2014 14:00]; Bray et al. (2015).

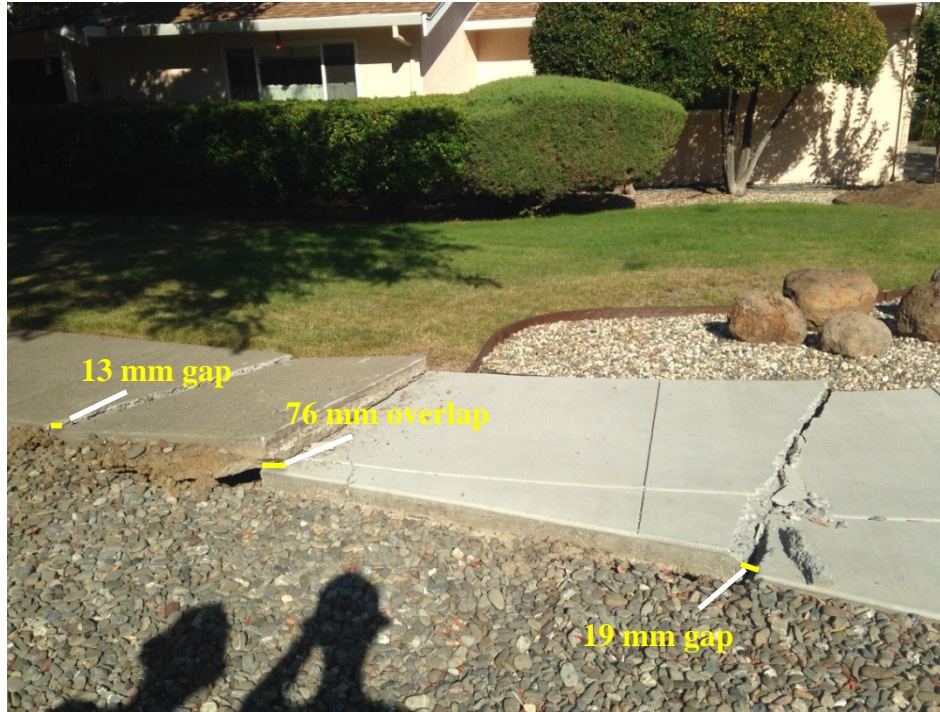


Figure 5: Measuring an overlapped compression zone with a gap in sidewalk pavement [N 38.3047 W 122.3459; 8/26/2014 16:52]; Bray et al. (2015).

Ground strain computations and map

Ground strain was computed over each 25 meter segment by adding the measured extension cracks (positive) and compression zones (negative) to the measured segment length to obtain the original segment length. This became the “gage length” of the strain measurement. Then, the difference between the measured and the estimated original length was divided by the estimated original length to obtain the decimal strain, which was converted to a percent strain. Additionally, the average strain for each sidewalk section as a whole was computed in a similar manner by considering all measured extension cracks and compression zones added to the total length of the segments of a single sidewalk. The results of the average strain over each total sidewalk are shown in Table 1 for sidewalks parallel and perpendicular to the fault. A schematic showing the approximate location of each extension crack and compression zone is shown in Figure 6.

Table 1: Summary of strain measurements (compression negative); Bray et al. (2015).

N-S (Parallel) Trending Roads			E-W (Orthogonal) Trending Roads		
Side of Fault	Average Strain (%)		Side of Fault	Average Strain (%)	
	East	West		North	South
West	-0.01	-0.03	West	-0.02	0.01
East	0.00	0.00	East	0.00	0.00
Crossing	0.01	0.36	Crossing	-0.24	-0.17

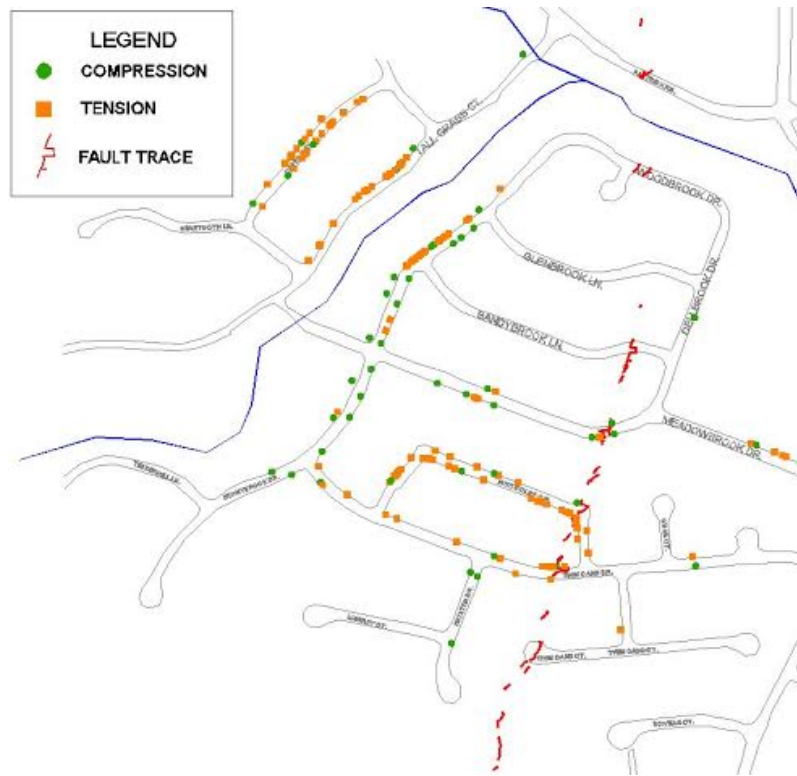


Figure 6: Observed and measured tension (orange squares) and compression (green circles) locations; Bray et al. (2015).

Additional Observations

In addition to the deformations in the concrete sidewalks compression features in the curb strip adjacent to the sidewalk, cracking in asphalt, damaged curbs, and a fence adjacent to the fault trace were measured and documented.

An interesting phenomenon were compression features in grass mats in the curb strips at various locations adjacent and parallel to the sidewalk pavement (Figure 7). Note the lack of apparent deformation in the adjacent concrete walk pavement while the grass mat buckled and actually shortened as a result of the buckling. This suggests that the concrete behaved elastically as the surface wave(s) traveled across this zone whereas the grass mat remained in its compressed state.

Permanent deformation was also observed on a section of a fence running parallel to and adjacent to the fault trace (Figure 8). To compute the strain, the horizontal boards at the top of the fence were measured in segments to obtain an estimate of the original length of the fence. Then, the ground along the base of the fence was measured to obtain an estimate of the new length of the fence. The average strain in the fence was the same order of magnitude as the average strain in the sidewalk pavement for roads crossing the fault trace.



Figure 7: Compression feature in curb strip parallel to fault, across from creek [N 38.3065 W 122.3455; 8/28/2014 13:52]; Bray et al. (2015).

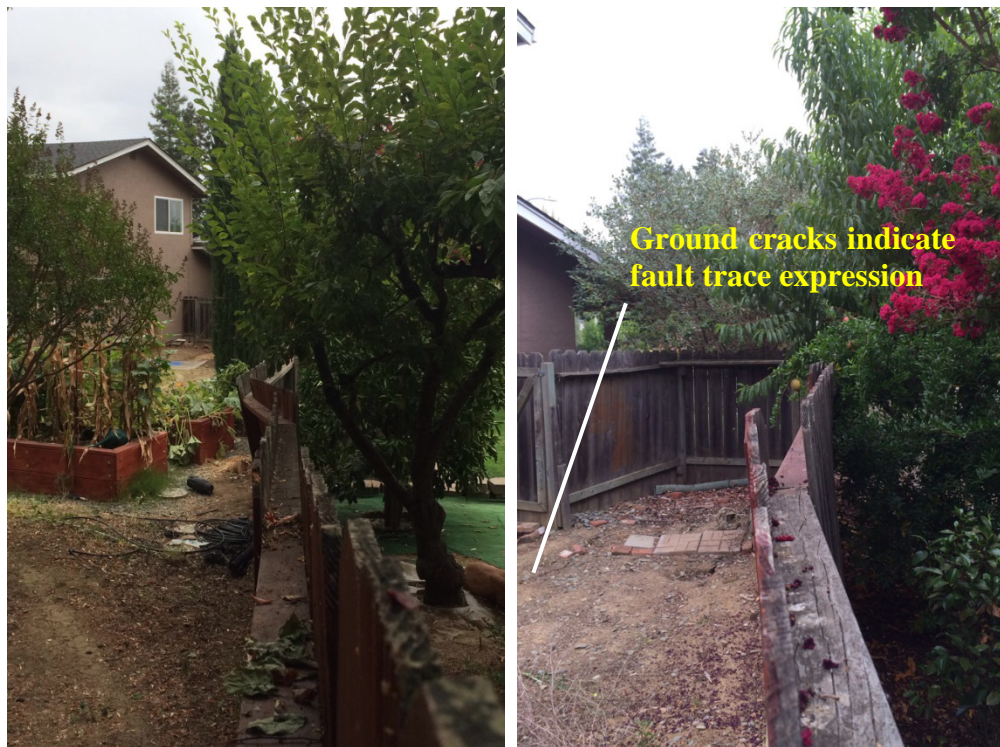


Figure 8: Buckled section of fence for strain measurements [N 38.3015 W 122.3442; 8/25/2014 09:57]; Bray et al. (2015).

One of the more enigmatic observations was that bituminous pavement was largely devoid of compression features except immediately along the fault trace. Most of the cracks in bituminous pavement were transverse to the direction of the street and appeared to be extensional. In addition, most manholes and other penetrations in the pavement were ringed by apparently fresh cracks.

Damaged curbs were observed throughout the neighborhood along roads both parallel and perpendicular to the fault trace. The damage included crushing, extension cracks and buckling failures. In general, the damaged curbs were not directly adjacent to the buckled compression zones in the sidewalk pavement. However, the curbs were not included in the detailed surveying because in most cases the broken pieces were missing or could not be reconstructed into the original configuration.

Conclusions

The August 24, 2014 M6.0 South Napa earthquake was the largest earthquake in the San Francisco Bay area since the October 17, 1989 M6.9 Loma Prieta earthquake. The most unusual and distinct damage were compressional and extensional failures of relatively new, stiff concrete sidewalks and curbs in the Browns Valley area. The observed alternating patterns of sidewalk compression zones and extension zones are quite unique as such features have not been recorded in the near fault regions of other earthquakes. Moreover, given the complexity of the site conditions, i.e. thin fill over bedrock in most of the area, it is not clear whether these features were caused by near fault surface waves or by some other form of ground deformation such as fill compaction or translation. Further study of these types of ground deformations in future earthquakes is warranted as it may be possible to obtain a better understanding of ground strain in the near fault environment. Finally, it should be noted that typical slab on grade foundations of the houses showed none of these effects, which only makes the observed behavior that much more enigmatic.

Acknowledgments

The response to the August 24, 2014 M6.0 South Napa, California earthquake was a collaborative effort with significant collaboration amongst members of the following organizations: California Geological Society, National Science Foundation sponsored Geotechnical Extreme Events Reconnaissance (GEER) Association, Pacific Earthquake Engineering Research Center (PEER), University of California, Berkeley and U.S. Geological Survey. The work of the GEER Association is based upon work supported in part by the National Science Foundation through the Geotechnical Engineering Program under Grant No. CMMI-1266418. Special thanks go to those who assisted with the field measurements: Heyder Carlosama, Julien Cohen-Waeber, Michael Gardner, Robert Lanzafame and Roberto Luque.

References

Bray, J., Cohen-Waeber, J., Dawson, T. Kishida, T. & Sitar, N. (2015). *Geotechnical Engineering Reconnaissance of the August 24, 2014 M6 South Napa Earthquake* (GEER Association Report No. GEER-037). Geotechnical Extreme Events Reconnaissance. Retrieved February 4, 2015, from http://www.geerassociation.org/GEER_Post%20EQ%20Reports/SouthNapa_2014/index.html